NASA TECHNICAL MEMORANDUM

NASA TM X-1613

NASA TM X-1613

ON ELECTROMAGNETIC SWITCHING PROPERTIES OF A BI-STABLE FLUIDIC ELEMENT WITH NON-DESTRUCTIVE MEMORY

by Joseph S. Koziol, Jr., and Robert De Furia

Electronics Research Center

Cambridge, Mass.

NATIONAL AERONAUTICS AND SPACE ADMINISTRATION • WASHINGTON, D. C. • AUGUST 1968

NASA TM X-1613

ON ELECTROMAGNETIC SWITCHING PROPERTIES OF A BI-STABLE FLUIDIC ELEMENT WITH NON-DESTRUCTIVE MEMORY

By Joseph S. Koziol, Jr., and Robert De Furia

Electronics Research Center
Cambridge, Mass.

NATIONAL AERONAUTICS AND SPACE ADMINISTRATION

For sale by the Clearinghouse for Federal Scientific and Technical Information
Springfield, Virginia 22151 – CFSTI price $3.00

ON ELECTROMAGNETIC SWITCHING PROPERTIES OF A BI-STABLE FLUIDIC ELEMENT WITH NON-DESTRUCTIVE MEMORY

By Joseph S. Koziol, Jr., and Robert De Furia
Electronics Research Center

SUMMARY

This report discusses the feasibility of controlling a magnetically permeable liquid bead with an electromagnet between two stable states of a particular system. Several useful properties of the switching system, namely, magnetomotive force required for switching, switching time, and ambient acceleration field limits are determined in terms of the system parameters.

This concept suggests a simple, bi-stable, low-power, electric-to-fluid transducer with non-descructive memory. (The fluid bead retains its last stable state with all power off.)

Development of a magnetically permeable liquid with high surface tension did not reach the stage for implementation, at the completion of the analysis, to permit experimental verification of the analytical results contained herein.

INTRODUCTION

The unique characteristics of fluidics offer many advantages over conventional methods for performing logic, sensing, amplifying, and actuating. Besides eliminating wear of moving parts, fluidic implementation is relatively impervious to damage by the environmental effects of radiation and high temperature. These considerations are especially important when designing systems for deep-space missions such as a space probe.

Recognition of these inherent advantages, per se, has not and will not be a panacea for realizing actual functioning systems. Although fluidic technology is expanding at a rapid pace, system development is still in its embryonic stage and many breakthroughs are needed. One such area of significance is the efficient conversion of electric signals to fluidic equivalents.

The purpose of this paper is to describe a system with this capability and to discuss the feasibility of its implementation.

The mechanism analyzed herein consists of a liquid bead which is geometrically retained in either of two stable states by its surface tension. In a typical system, each state could serve as a control port for gas flow.

This concept of controlling a gas flow by means of a liquid bead has been labelled, perhaps inappropriately, two-phase fluidics. It was developed by the Conrac Corporation and now provides a basis for research on a number of fluidic components. Its usefulness has already been demonstrated by the successful operation of an alpha-numeric display with memory (refs. 1 and 3) and by an infinite-input impedance amplifier (ref. 2). In these two applications, control of the liquid bead was accomplished by pressure signals. This report considers control of a magnetically permeable liquid bead by means of an electromagnet; hence, suggesting possible applications as an electric to fluid transducer.

This report evolved from previous research originated by the Conrac Corporation (formerly Giannini Controls Corporation) under Contract NAS 12-43 with NASA-ERC (refs. 1 and 2).

SYMBOLS

A	cross-section area of electromagnet, $meter^2$
A_B	surface area of bead, $meter^2$
A_o	initial surface area of bead, $meter^2$
B	magnetic field intensity, $weber/meter^2$
D	height of electromagnet gap, meter
F_B	electromagnetic force, (amp-turn) weber/meter
F_{ST}	surface force, newton
g	earth's gravitational constant, $meter/sec^2$
g_a	ambient acceleration field factor, dimensionless
H	bead dimension, meter
I	current, ampere
kg	kilogram
ℓ	electromagnet length, meter
L	restriction length, meter
M	mass of bead, kilogram
N	number of turns of coil

NI,MMF	magnetomotive force, amp-turn
r	radius of restriction, meter
R	radius of chamber, meter
$\mathcal{R}, \mathcal{R}_g, \mathcal{R}_1$ $\mathcal{R}_2, \mathcal{R}_3, \mathcal{R}_4$	reluctance, ampere/weber
t	time, second
t_s	switching time, second
T	kinetic energy, newton-meter
U	potential energy, newton-meter
U_B	electromagnetic potential energy, (amp-turn) weber
U_{BO}	electromagnetic energy constant, (amp-turn) weber
U_{ST}	surface potential energy, newton-meter
U_{STO}, $\overline{U}_{STO}$	surface energy constant, newton-meter
U_g	electromagnetic energy in gap, (amp-turn) weber
W	electromagnet width, meter
x	independent coordinate, center-of-mass position of bead, meter
x_L	position of bead's leading surface, meter
x_o	geometric center of switching system, meter
x_{SW}	position of center-of-mass at switching, meter
$\dot{x}$	velocity of bead's center-of-mass, meter/sec
$\ddot{x}$	acceleration of bead's center-of-mass, meter/sec^2
ρ	density of bead, kg/meter^3
ϕ	magnetic flux, weber
σ	surface tension constant, newton/meter

μ	magnetic permeability of electromagnet, weber/amp-meter
μ_b	magnetic permeability of bead, weber/amp-meter
μ_g	magnetic permeability of body in electromagnet gap, weber/amp-meter
μ_o	magnetic permeability of air, weber/amp-meter

ANALYSIS

The generalized Lagrange equation is a convenient method for analyzing the dynamic behavior of discrete point systems especially when the system can be described in terms of independent coordinates. It will be used to describe the motion of a magnetically permeable liquid bead constrained to move through a restriction while influenced by a magnetic field. The general representation of such a system is shown in Figure 1.

In analyzing the bead's motion, emphasis will be placed on the center-of-mass of the bead, while the deformation of the bead will be assumed to affect only the potential energy. In other words, the bead is treated as a rigid body with its kinetic energy balanced by the electromagnetic energy of the applied "B" field and surface energy, or work done by the surface tension, which is implemented by the variable restriction.

A strict energy description of the problem would require representing the variational motions of each individual segment of the fluid bead with properly defined coordinates and constraints.

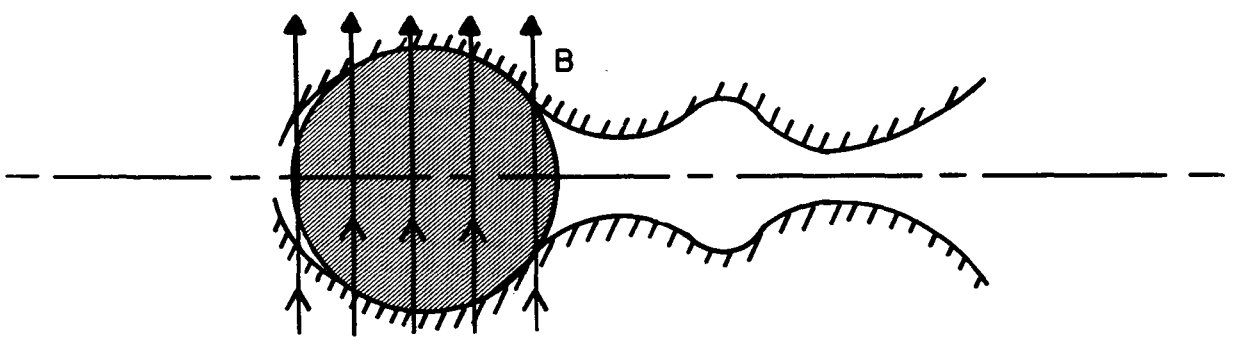

Figure 1.-General representation of a magnetically permeable bead in a variable restriction with applied magnetic field "B"

However, since the main point of interest is not to examine the fluid flow phenomena involved, but rather to follow the macroscopic displacement of the bead, the net effect will be represented in terms of its center-of-mass motion.

This approach allows the problem to be described in terms of a single independent coordinate, namely, the motion of the bead center-of-mass.

The Lagrange equation for one independent coordinate, x, is given by:

$$\frac{d}{dt}\left(\frac{\partial T}{\partial \dot{x}}\right) - \frac{\partial (T - U)}{\partial x} = 0 \qquad (1)$$

where T and U are the total kinetic and potential energies of the system, respectively.

No generalized force is included on the right-hand side of this equation, since the applied electromagnetic force arises from a potential. The potential energy U, thus, consists of the surface tension energy and the electromagnetic energy.

In order to proceed further in the analysis, a specific system needs to be defined. The system chosen for this report, shown in Figure 2, lends itself to a simple description of the restriction parameters and is not intended to suggest an optimum design.

The origin of the coordinate system is established at the bead's initial center-of-mass position when the bead is just about to enter the restriction, while "x_o" is the distance to the system's geometric center from the origin.

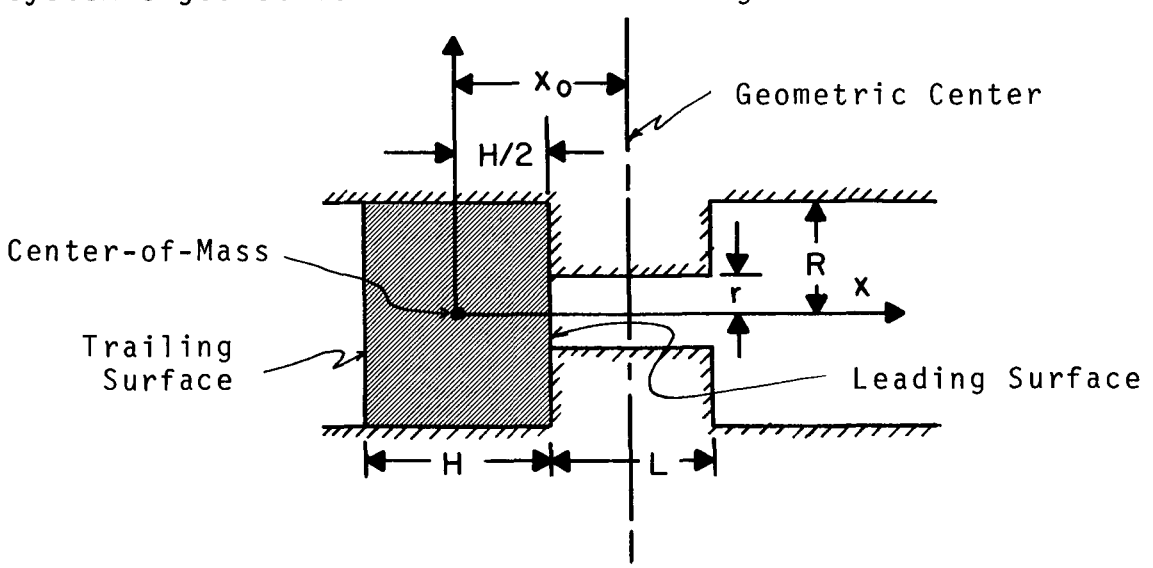

Figure 2.-System configuration

An electromagnetic energy approximation and a surface tension energy approximation have been developed in Appendices A and B, respectively, for a certain switching model of the system shown in Figure 2. These approximations are repeated here for convenience. The electromagnetic energy approximation is:

$$U_B = U_{BO} + F_B x \tag{2}$$

where

$$U_{BO} = -\frac{1}{2}(NI)^2 \left\{ \left[\mu_o \left(1-\frac{r}{R}\right)(2R+L) \right] + \left[\mu_o \frac{r}{R}(2R+L) \right] + \left[\frac{\frac{r^2}{R^2}(\mu_b-\mu_o)}{\frac{r}{R} + \frac{\mu_b}{\mu_o}\left(1-\frac{r}{R}\right)} \right] \frac{H}{2} \right\} \tag{3}$$

$$F_B = \left[\frac{\frac{r^2}{R^2}(\mu_b-\mu_o)}{\frac{r}{R} + \frac{\mu_b}{\mu_o}\left(1-\frac{r}{R}\right)} \right] \left\{ \frac{2\left(\frac{R}{r}-1\right)\left(\frac{H+L}{2}\right) - H\left(\frac{R}{r}+1\right)}{2\,\frac{R}{r}\left[1-\left(\frac{r}{R}\right)^3\right]\left[\frac{H+L}{2}\right]} + \frac{\sqrt{H^2\left(\frac{R}{r}+1\right)^2 + 4H\left[2\left(\frac{R}{r}\right)^3 - \left(\frac{R}{r}\right)^2 - 1\right]\left[\frac{H+L}{2}\right] + 4\left(\frac{R}{r}-1\right)^2\left(\frac{H+L}{2}\right)^2}}{2\,\frac{R}{r}\left[1-\left(\frac{r}{R}\right)^3\right]\left[\frac{H+L}{2}\right]} \right\} \tag{4}$$

μ_b and μ_o are the magnetic permeabilities of the bead and air, respectively.

The surface energy approximation is:

$$\begin{aligned} U_{ST} &= U_{STO} + F_{ST}x \qquad && x \le x_o \\ &= \overline{U}_{STO} - F_{ST}x \qquad && x \ge x_o \end{aligned} \tag{5}$$

where

$$U_{STO} = 2\pi R\sigma(R + H) \tag{6}$$

$\overline{U}_{STO}$ = energy constant determinable from Figure B-4

$$F_{ST} = \frac{2\pi R\sigma\left(\frac{R}{r}-1\right)}{\left(\frac{R}{r}\right)^3 - 1}\left\{\left(\frac{R}{r}-1\right) - \frac{H\left(\frac{R}{r}+1\right)}{H+L} + \sqrt{H^2\left(\frac{\frac{R}{r}+1}{H+L}\right)^2 + \frac{2H}{H+L}\left[2\left(\frac{R}{r}\right)^3 - \left(\frac{R}{r}\right)^2 - 1\right] + \left(\frac{R}{r}-1\right)^2}\right\} \tag{7}$$

and

$$x_o = \frac{H + L}{2} = \text{geometric center.} \tag{8}$$

The kinetic energy of the bead is:

$$T = \frac{1}{2} M\dot{x}^2 \tag{9}$$

where M is the mass of the bead and $\dot{x}$ is the velocity of the bead's center-of-mass.

When these equations are substituted into Eq. (1), the equation describing the behavior of the bead becomes

$$\begin{aligned} M\ddot{x} &= -F_B - F_{ST} \qquad && x \le x_o \\ &= -F_B + F_{ST} \qquad && x \ge x_o \quad . \end{aligned} \tag{10}$$

The value of $-F_B$ is positive, since F_B is negative and represents the electromagnetic driving force contribution resulting from an applied magnetomotive force, NI.

The quantity $-F_{ST}$ represents a constant restraining force as the bead enters the restriction ($x \leq x_o$) and F_{ST} represents an equal propelling force when it emerges ($x \geq x_o$).

The solution of Eq. (10) describes a single switching process and assumes that friction is negligible. Further, the switching process is treated as symmetrical and reversible; thus, impact effects are neglected.

The solution of Eq. (10) is valid only when the right-hand side of the first equation is positive. Otherwise, the applied electromagnetic force, $-F_B$, is less than the surface tension restraining force and the bead will not switch. In this case, the bead has no motion and any applied electromagnetic force is balanced by a wall-restraining force.

When the applied electromagnetic force is equal to the surface tension restraining force, the bead is on the verge of switching, and this defines the electromagnetic force required for switching.

If the applied electromagnetic force is greater than the electromagnetic force required for switching, then switching time can be determined from solution of Eq. (10).

The determination of the ambient acceleration field that will cause switching without an applied electromagnetic force will provide a third characteristic of the system.

These three characteristics, when related to the system parameters, would provide valuable design information. They will now be examined separately.

Electromagnetic Force Required for Switching

The electromagnetic force required for switching can be determined, by definition, from the following equation.

$$-F_B = F_{ST} \tag{11}$$

Substituting from Eqs. (4) and (7) and rearranging the equation in normalized form gives:

$$\left[\frac{\mu_o}{4\pi R\sigma}\right]^{1/2}(NI) = \left\{\frac{\left(\frac{\mu_o}{\mu_b} - 1 + \frac{R}{r}\right)\left(1 - \frac{r}{R}\right)}{1 - \frac{\mu_o}{\mu_b}}\right\}^{1/2} \qquad (12)$$

where NI is the magnetomotive force.

This curve is plotted in Figure 3 as a function of the restriction r/R. It can be seen that the magnetomotive force required for switching is independent of the size of the bead, H/R, the restriction length, L/R, and the permeability ratio, μ_b/μ_o (for $\mu_b/\mu_o > 100$).

As would be expected, the electromagnetic force required for switching decreases with larger restrictions. The curve also shows that for blocked restrictions (i.e., r/R = 0), it is impossible to switch the bead, and for no restriction (i.e., r/R = 1), the bead can switch without an applied magnetomotive force.

Switching Time

It is first necessary to define "switching." "Switching" will be defined to have occurred when the trailing surface (see Figure 2) reaches the restriction. Switching time can now be determined from the dynamic solution of Eq. (10).

Substituting from Eqs. (4) and (7), solving, and normalizing properly gives:

$$\frac{t_s}{2R\sqrt{\frac{\rho R}{\sigma}}} = \left\{\left(\frac{R}{r}-1\right)\left(\frac{H}{R} + \frac{L}{R}\right) \Bigg/ \left[\frac{\mu_o}{8\pi R\sigma}(NI)^2 \frac{\left(\frac{\mu_b}{\mu_o}-1\right)\frac{R}{r}}{1 + \frac{\mu_b}{\mu_o}\left(\frac{R}{r}-1\right)}\right.\right.$$

$$\left.\left. + \frac{R}{r} - 1\right]\right\}\left\{\frac{H}{2R}\left(\frac{R^3}{r^3}-1\right) \Bigg/ \left[\left\{\frac{\mu_o}{8\pi R\sigma}(NI)^2 \frac{\left(\frac{\mu_b}{\mu_o}-1\right)\frac{R}{r}}{1 + \frac{\mu_b}{\mu_o}\left(\frac{R}{r}-1\right)}\right.\right.\right. \qquad \text{(contd)}$$

$$- \frac{R}{r} + 1\Bigg\}\Bigg\{\left(\frac{R}{r}-1\right)\left(\frac{H}{R} + \frac{L}{R}\right)\frac{H}{R}\left(\frac{R}{r}+1\right) + \Bigg[\left(\frac{H}{R}\right)^2\left(\frac{R}{r}+1\right)^2 + 4\,\frac{H}{r}\Bigg[2\left(\frac{R}{r}\right)^3$$

$$- \left(\frac{R}{r}\right)^2 - 1\Bigg]\left(\frac{H+L}{2R}\right) + 4\left(\frac{R}{r}-1\right)^2\left(\frac{H+L}{2r}\right)^2\Bigg]^{\frac{1}{2}}\Bigg\}\Bigg]\Bigg\}^{\frac{1}{2}}$$

$$\left\{1 \pm \left[\left(\frac{\mu_o}{8\pi R\sigma}(NI)^2\,\frac{\left(\frac{\mu_b}{\mu_o}-1\right)\frac{R}{r}}{1 + \frac{\mu_b}{\mu_o}\left(\frac{R}{r}-1\right)} - \frac{R}{r} + 1\right)\right. \qquad (13)$$

$$\left(\frac{\mu_o}{8\pi R\sigma}(NI)^2\,\frac{\left(\frac{\mu_b}{\mu_o}-1\right)\frac{R}{r}}{1 + \frac{\mu_b}{\mu_o}\left(\frac{R}{r}-1\right)}\left(\frac{H}{2R} + \frac{R^2}{r^2}\,\frac{H}{2r}\right)\right.$$

$$\left.\left.\left. + \left(\frac{R}{r}-1\right)\left(\frac{H}{2r}\,\frac{R^2}{r^2} - \frac{H}{2r} - L\right)\right) \Bigg/ 2\left(\frac{H}{R} + \frac{L}{R}\right)\left(\frac{R}{r}-1\right)^2\right]^{\frac{1}{2}}\right\}$$

Plots of Eq. (13) are shown in Figures 4, 5, and 6 as functions of the applied magnetomotive force. The vertical asymptotes are the magnetomotive forces required for switching for each respective restriction.

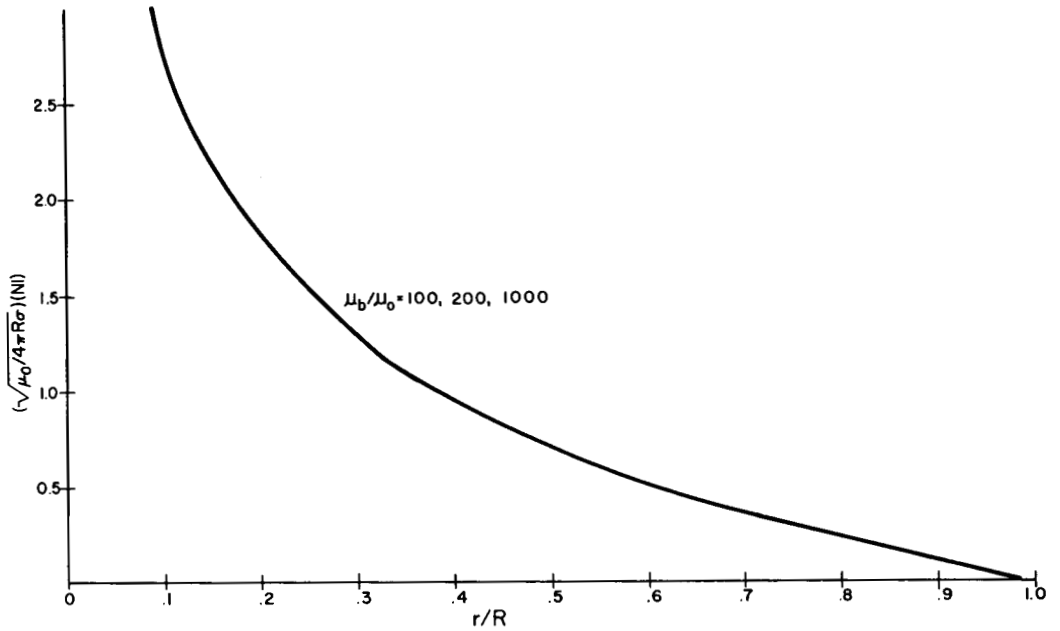

Figure 3.-Magnetomotive force required for switching vs. restriction size

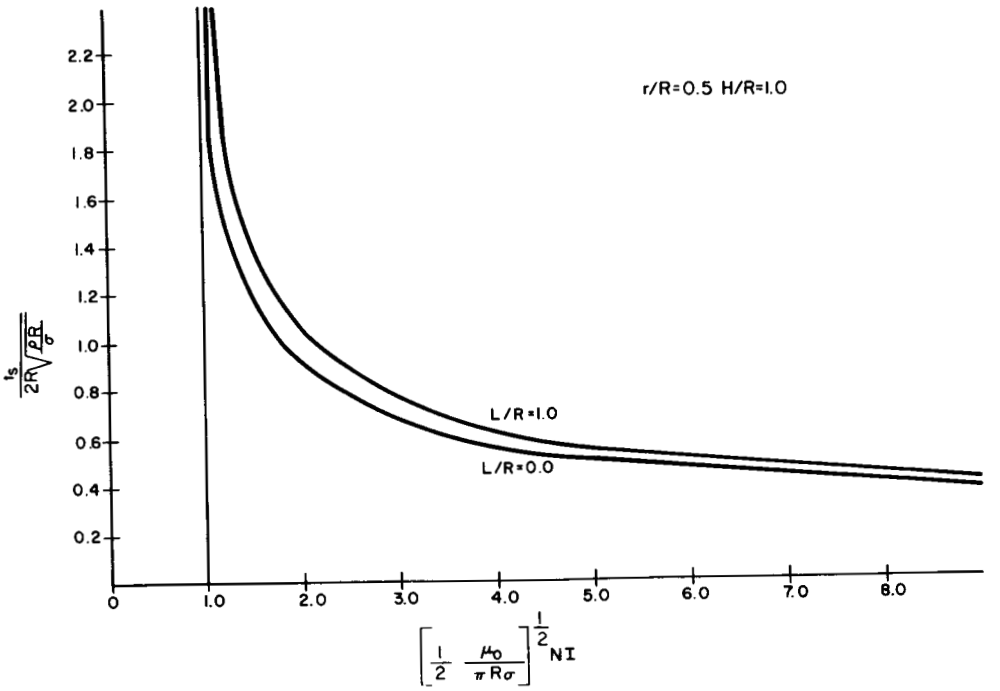

Figure 4.-Switching time vs. applied magnetomotive force showing the effect of restriction length

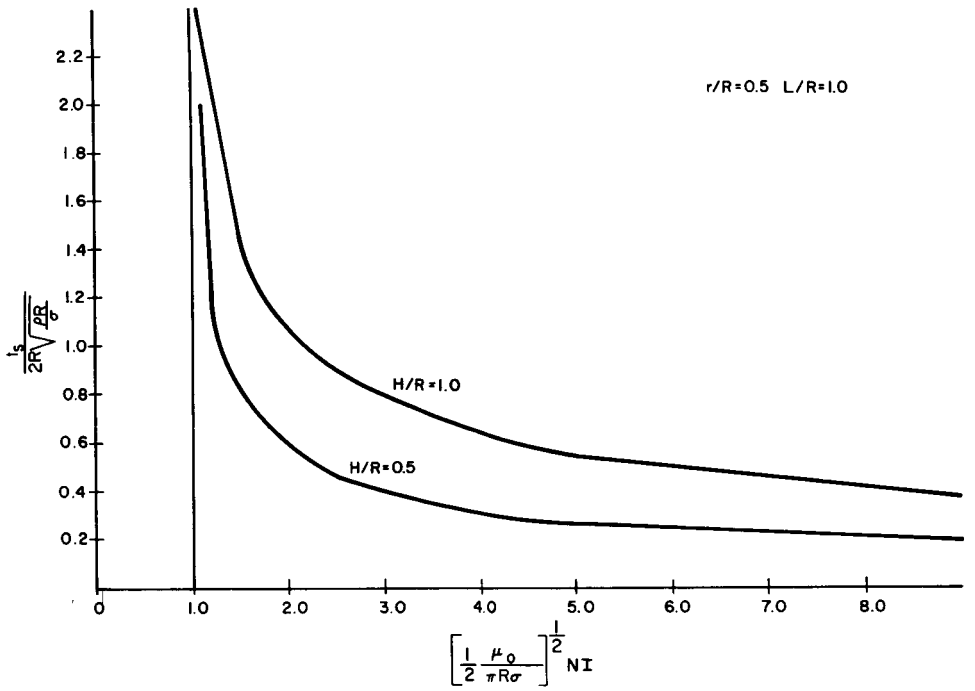

Figure 5.-Switching time vs. applied magnetomotive force showing the effect of the bead's size

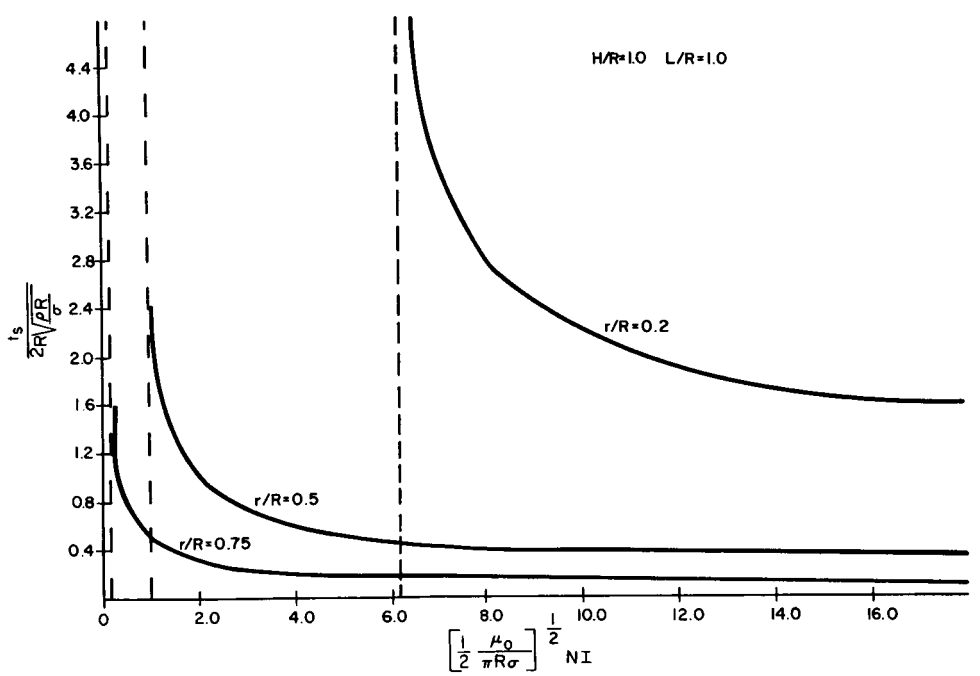

Figure 6.-Switching time vs. applied magnetomotive force showing the effect of restriction size

As would be expected, for a given restriction, higher applied magnetomotive forces result in lower switching times.

Figure 4 shows that the effect of restriction lengths is negligible for $L/R < 1$.

Figure 5 shows that the size of the bead can reduce the switching time significantly.

Figure 6 shows that for a given applied magnetomotive force larger than that required for switching, the switching time decreases significantly with larger restrictions.

Ambient Acceleration Field Limit

It is possible that ambient acceleration fields could cause unwanted switchings without an applied magnetomotive force. The axial acceleration field component that would cause such switching can be determined from Eq. (10) with the magnetomotive force set equal to zero.

Substituting from Eq. (7) and normalizing properly gives:

$$\frac{g_a}{\left(\frac{4\sigma}{R^2\rho g}\right)} = \frac{\frac{R}{r} - 1}{2\left(\frac{H}{R}\right)\left[\left(\frac{R}{r}\right)^3 - 1\right]} \left\{ \left(\frac{R}{r}-1\right) - \frac{\frac{H}{R}\left(\frac{R}{r}+1\right)}{\frac{H}{R} + \frac{L}{R}} \right.$$

$$+ \left[\left(\frac{H}{R}\right)^2 \left(\frac{\frac{R}{r} + 1}{\frac{H}{R} + \frac{L}{R}}\right)^2 + \frac{2\,\frac{H}{r}}{\left(\frac{H}{R} + \frac{L}{R}\right)} \left[2\left(\frac{R}{r}\right)^3 - \left(\frac{R}{r}\right)^2 - 1 \right] \right.$$

$$\left. \left. + \left(\frac{R}{r}-1\right)^2 \right]^{\frac{1}{2}} \right\} \qquad (14)$$

Equation 14 is plotted in Figure 7 as a function of the restriction, r/R.

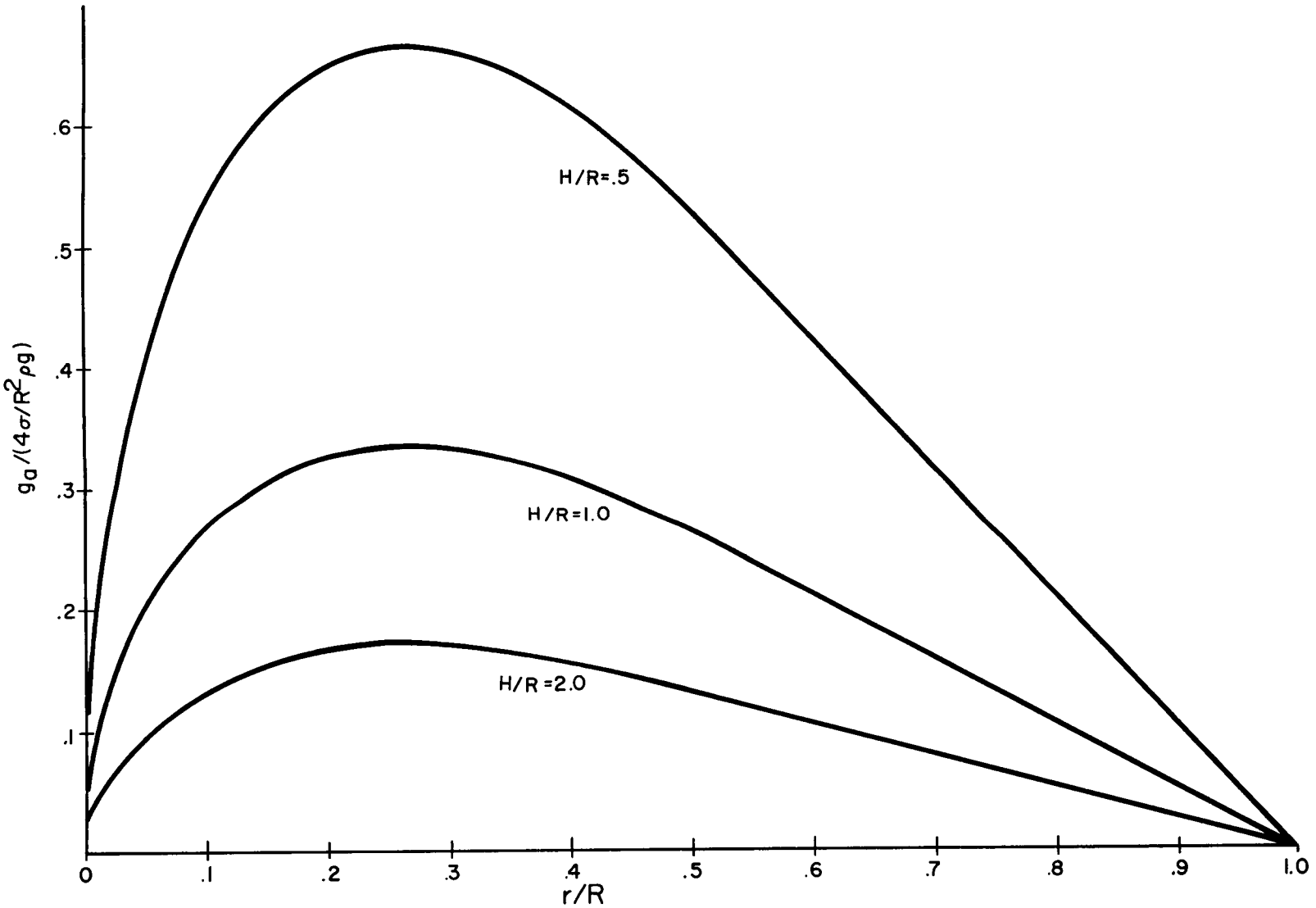

Figure 7.-Ambient acceleration field limit vs. restriction size

It is apparent that the curves are not valid for $r/R < .25$. This can be accounted for by an increased error resulting from the surface tension energy approximation in this region. (See Appendix B.)

Otherwise, it can be seen that the axial acceleration field limit is independent of the restriction length and inversely related to the size of the bead. Also, as would be expected, the bead could switch with virtually no ambient acceleration field present when $r/R = 1$.

Numerical Example

A numerical example is provided here to show that the predicted values of magnetomotive force required for switching, switching time, and axial acceleration field limit are practical. Consider a typical system with the following parameters:

$L/R = 1.0, \quad r/R = 0.5$

$S/R = 1.0$

$\mu_b/\mu_o = 200$

$\mu_o = 4\pi \times 10^{-7}$ weber/amp-meter

$R = 3.0 \times 10^{-3}$ meter

$\sigma = .462$ newton/meter

$\rho = 13.5 \times 10^3$ kg/m^3

Magnetomotive force required for switching.- From Figure 3:

$$\left[\frac{\mu_o}{4\pi R\sigma}\right]^{\frac{1}{2}} (NI) = .72$$

$$(NI) = 88 \text{ amp-turns.}$$

For $N = 1000$, and a resistance in the coil equal to 1 ohm, the power expended during switching is .0077 watt.

Switching time.- From Figure 5 and with an applied magnetomotive force of 200 amp-turns:

$$\frac{t_s}{2R\sqrt{\frac{\rho R}{\sigma}}} = .94$$

$$t_s = .051 \text{ second.}$$

If the applied magnetomotive force were increased to 500 amp-turns, the switching time would be reduced to only .028 second.

Ambient acceleration field limit.- From Figure 7:

$$\frac{g_a}{\left(\frac{4\sigma}{R^2\rho g}\right)} = .263$$

$$g_a = .44 \text{ g's.}$$

CONCLUSIONS

Several useful properties of the electromagnetic switching system have been determined in terms of the system parameters. These properties are magnetomotive force required for switching, switching time, and ambient acceleration field limit.

The results of the numerical example predict that the system could perform quite satisfactorily as a low-power, digital, electric-to-fluid transducer.

It is quite difficult to otherwise appraise this system without experimental data. Several assumptions were made in the development and could be validated by actual experimentation. However, the development of a proper fluid bead has not yet reached the stage for final implementation of this concept. Experiments with various materials for developing a non-wetting liquid with high magnetic permeability and high surface tension are progressing in this Center.

The results of this report are not valid for small restrictions, first of all, because of the approximation method adopted. (See Appendix B.) Also, the actual switching model equation omits the effects of friction and hysteresis which would be significant for small restrictions.

No attempt was made to perform an accurate small restriction analysis because such a system appears to be impractical. In addition, the analysis would require a much more complicated model to describe the behavior of the bead which would be subject to greater possibilities of rupture.

Regardless of these comments, the fluid bead concept itself might suggest other applications and thereby warrants further research to expand fluidic technology.

The fabrication of a proper liquid bead is a primary need. The required properties include high magnetic permeability, non-wetting capabilities, and high surface tension. True fluids having high magnetic permeability have been developed but these are wetting fluids and, therefore, unsuitable for this application (refs. 4 and 5). In most cases, they are corrosive, highly volatile, and prone to oxidation. Also, surface tension is often treated as a property of liquids, though it is actually a property of the boundary of the liquid and cannot be given an exact value without specifying the material which lies on the other side of the boundary. Hence, development of the bead material cannot be separated from that of the system material.

Other germane research areas could include optimization of the restriction geometry to allow switching with minimum power consumption and optimization of performance (i.e., quickest switching without damage) by application of bang-bang control to the applied magnetomotive force.

REFERENCES

1. Reader, T.D., and Ho, S.K.: Research on a Non-Destructive Fluidic Storage Control Device. Contract NAS 12-43, NASA CR-783, Giannini Report #ARD-FR-01-048-013, May 1966.
2. Martinez, E.: Development of an Infinite-Input-Impedance Fluidic Amplifier. Contract NAS 12-43, NASA CR-80023, June 1967.
3. Belsterling, C.A.: A Fluidic Digital Computer with Non-Destructive Memory. SAE Committed A-6 Symposium on Fluidics, San Francisco, California, October 1966.
4. Rosensweig, R.E.: Magnetic Fluid. Internation Science and Technology, July 1966.
5. Resler and Rosensweig.: Ferrohydrodynamic Fluids. American Institute of Chemical Engineers Eng. Symp. Series 5, Vol. 104, June 1965.

APPENDIX A

DERIVATION OF ELECTROMAGNETIC ENERGY MODEL AND APPROXIMATION

In simple magnetic circuits, as shown in Figure A.1, there is a formal analogy to Ohm's law for electric circuits given by:

$$MMF = R\phi \tag{A.1}$$

where MMF is the magnetomotive force analogous to electromotive force, R is the reluctance of the material in the circuit analogous to resistance, and ϕ is the flux analogous to current.

The magnetomotive force may be regarded as the agent that establishes the flux. The source of the magnetomotive force is the current flowing in the coil wound around the core of the magnet and is given by:

$$MMF = NI \tag{A.2}$$

where N is the number of turns of the coil and I is the current in the coil. The dynamics of the electronic circuit are neglected.

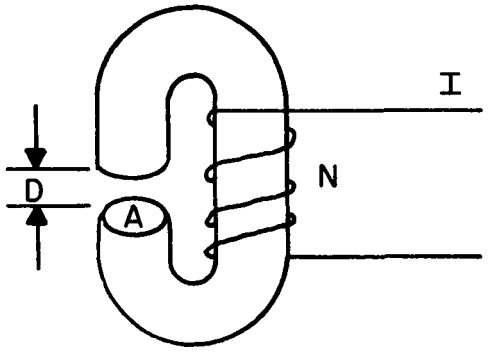

Figure A.1.-Electromagnet

Reluctance is defined as the ratio of magnetomotive force to the flux it produces. For a straight bar of uniform cross-section A, and length D, through which the flux lines are straight, parallel, and uniformly distributed (no fringing), the reluctance is given by:

$$R = \frac{D}{\mu A} \tag{A.3}$$

in which μ is the magnetic permeability of the material.

Since the permeability of the ferromagnetic core is much larger than the air or vacuum gap, the total reluctance of the magnetic circuit can be reasonably approximated by:

$$R_g = \frac{D}{\mu_g A} \tag{A.4}$$

in which μ_g is the permeability of the material in the gap, as long as D is small.

Combining the above equations:

$$NI = R_g \phi \quad . \tag{A.5}$$

The energy in the gap can also be expressed in terms of the reluctance of the magnetic path. With non-linearity and hysteresis neglected, the energy is:

$$U_g = -\frac{1}{2} \phi^2 R_g \quad . \tag{A.6}$$

Now if a body of permeability μ_g is placed in the gap, as shown in Figure A.2, the equivalent reluctance of the circuit and the energy in the gap will be affected.

The equivalent reluctance in the gap analogous to electronic circuitry becomes that of two reluctances, $D/(\mu_g Wx)$ and $D/[\mu_o W(\ell-x)]$ acting in parallel, namely:

$$R_g = \frac{D}{\ell W}\left[\frac{1}{\mu_g\left(\frac{x}{\ell}\right) + \mu_o\left(1-\frac{x}{\ell}\right)}\right] \tag{A.7}$$

where the area in the gap is now assumed rectangular and W is the width and ℓ is the length.

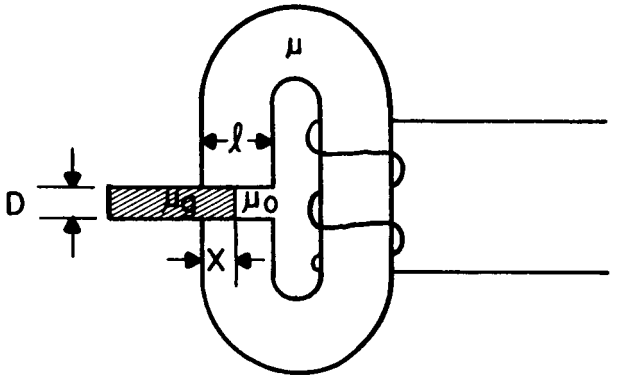

Figure A.2.-Electromagnet showing body (with permeability μ_g) partially in gap

This is also equivalent to the reluctance of the entire circuit if:

$$\mu \gg \mu_g \quad . \tag{A.8}$$

From Eq. (A.6) the energy in the gap is:

$$U_g = -\frac{1}{2}\phi^2 R_g = -\frac{1}{2}(NI)^2 \Big/ R_g \tag{A.9}$$

or:

$$U_g = -\frac{1}{2}(NI)^2 \frac{W}{D}\left[\mu_g x + \mu_0(\ell - x)\right] \quad . \tag{A.10}$$

A similar process can be followed in determining the energy in the restriction of the system shown in Figure A.3.

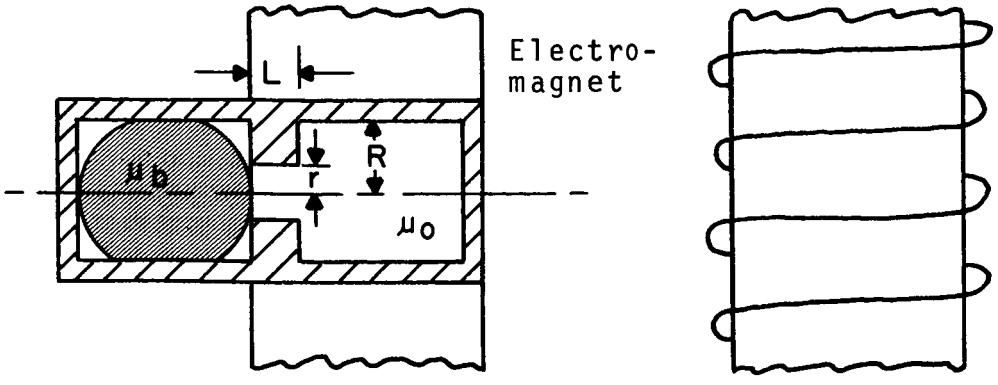

Figure A.3.-Complete switching system

In this configuration, the equivalent reluctance consists of parallel and series combinations schematically represented in Figure A.4.

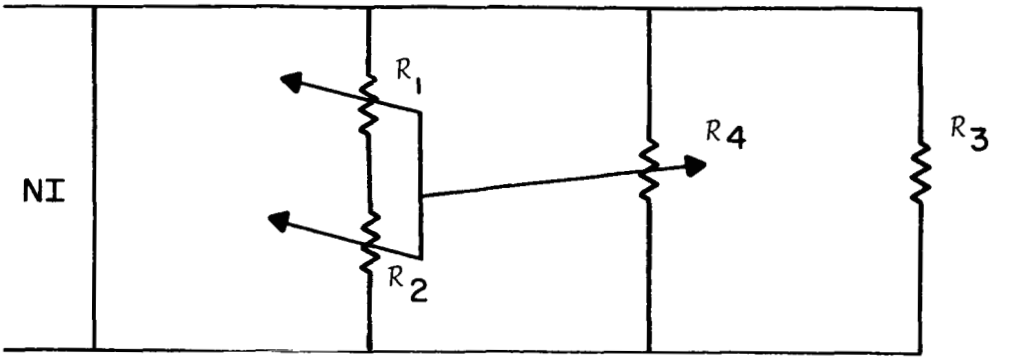

Figure A.4.-Schematic of Electromagnetic Circuit

The reluctances are defined as follows:

$$\mathcal{R}_1 = \frac{2r}{2\mu_b x_L r} = \frac{1}{\mu_b x_L} \tag{A.11}$$

$$\mathcal{R}_2 = \frac{2(R-r)}{2\mu_o x_L r} = \frac{R-r}{\mu_o x_L r} \tag{A.12}$$

$$\mathcal{R}_3 = \frac{2R}{2\mu_o (R-r)(2R+L)} = \frac{R}{\mu_o (R-r)(2R+L)} \tag{A.13}$$

$$\mathcal{R}_4 = \frac{2R}{2\mu_o r(2R+L-x_L)} = \frac{R}{\mu_o r(2R+L-x_L)} \tag{A.14}$$

where μ_b and μ_o are the magnetic permeabilities of the bead and air, respectively, x_L is the position of the leading surface, and L is the restriction length.

These equations assume that the permeability of the material containing the bead is approximately equal to that in the empty cavity (air) and that the bead has a flat leading surface.

Only one electromagnet is shown in Figure A.3, whereas in the actual system a second electromagnet, for reverse switchings, would be arranged similarly on the left side but rotated 90 degrees about the switching axis to prevent mechanical interference.

When the equivalent reluctance is determined and combined with Eq. (A.9), the energy in the restriction becomes:

$$U_B = -\frac{1}{2}(NI)^2\left\{\left[\mu_o\left(1-\frac{r}{R}\right)(2R+L)\right] + \left[\mu_o\frac{r}{R}(2R+L-x_L)\right] + \left[\frac{\mu_b\mu_o r x_L}{r\mu_o + \mu_b(R-r)}\right]\right\} \quad . \tag{A.15}$$

Equation (A.15), therefore, relates the electromagnetic potential energy of the bead to the position of its leading surface x_L, as the bead proceeds through the restriction. The form of Lagrange's equation in the text requires that the potential energy be expressed as a function of the independent coordinate, namely, the position of the bead's center-of-mass.

The position of the bead's leading surface can be related to its center-of-mass position by imposing the constant volume constraint. This gives:

$$x_L = \left\{\left[2\left(\frac{R}{r}-1\right)x - H\left(\frac{R}{r}+1\right) + \left[H^2\left(\frac{R}{r}+1\right)^2 + 4H\left[2\left(\frac{R}{r}\right)^3 - \left(\frac{R}{r}\right)^2 - 1\right]x + 4\left(\frac{R}{r}-1\right)^2x^2\right]^{\frac{1}{2}}\right] \Big/ 2\frac{R}{r}\left(1-\frac{r^3}{R^3}\right)\right\} + \frac{H}{2} \tag{A.16}$$

where x_L and x are defined from the origin of the coordinate system as shown in Figure A.5. The origin of the coordinate system is established at the bead's initial center-of-mass position when the bead is just about to enter the restriction.

Now consider the bead as it exits the restriction. If the switching process resembled the "squirt" model shown in Figure A.6, the relationship between the position of the bead's leading surface and its center-of-mass position would still be described by Eq. (A.16). However, deviations from the "squirt" switching model lead to different x_L vs. x relationships.

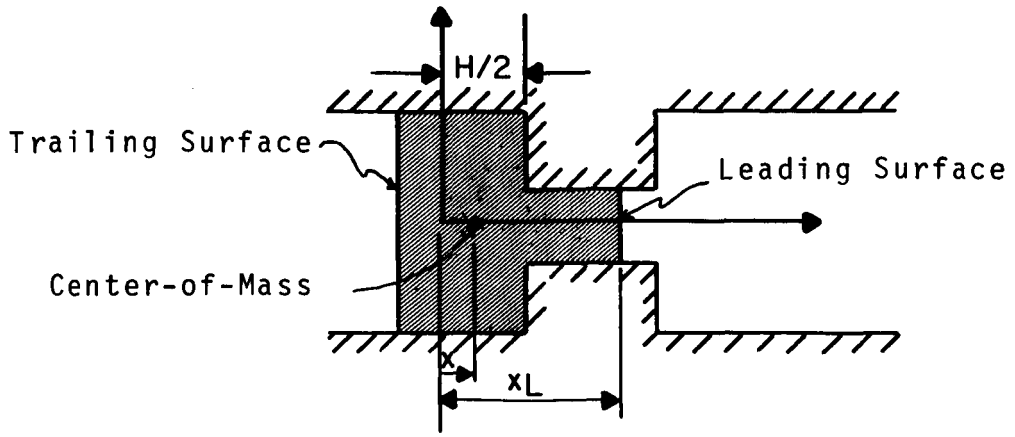

Figure A.5.-Bead configuration showing leading surface, trailing surface, and center-of-mass

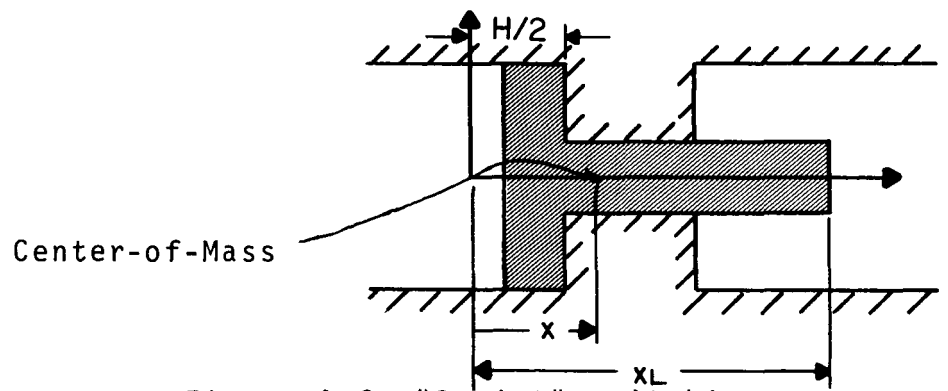

Figure A.6.-"Squirt" switching process model

The bounds of any possible x_L vs x relationship can be represented quite simply with respect to the "squirt" model. Equation (A.16) is plotted in Figure A.7 as solid lines for several restriction sizes. The leading surface position is the ordinate and the center-of-mass position is the abscissa.

Note that each curve can be approximated by a straight line quite well as x/R becomes large.

Now for each respective restriction, the solid line represents the maximum values of x_L that are physically possible.

Conversely, the straight line of slope "1" would represent the minimum values of x_L that are physically possible for any restriction (i.e., the center-of-mass and leading surface have no relative motion). The straight line of slope "1" also represents the only possible x_L vs. x relationship when r/R = 1.

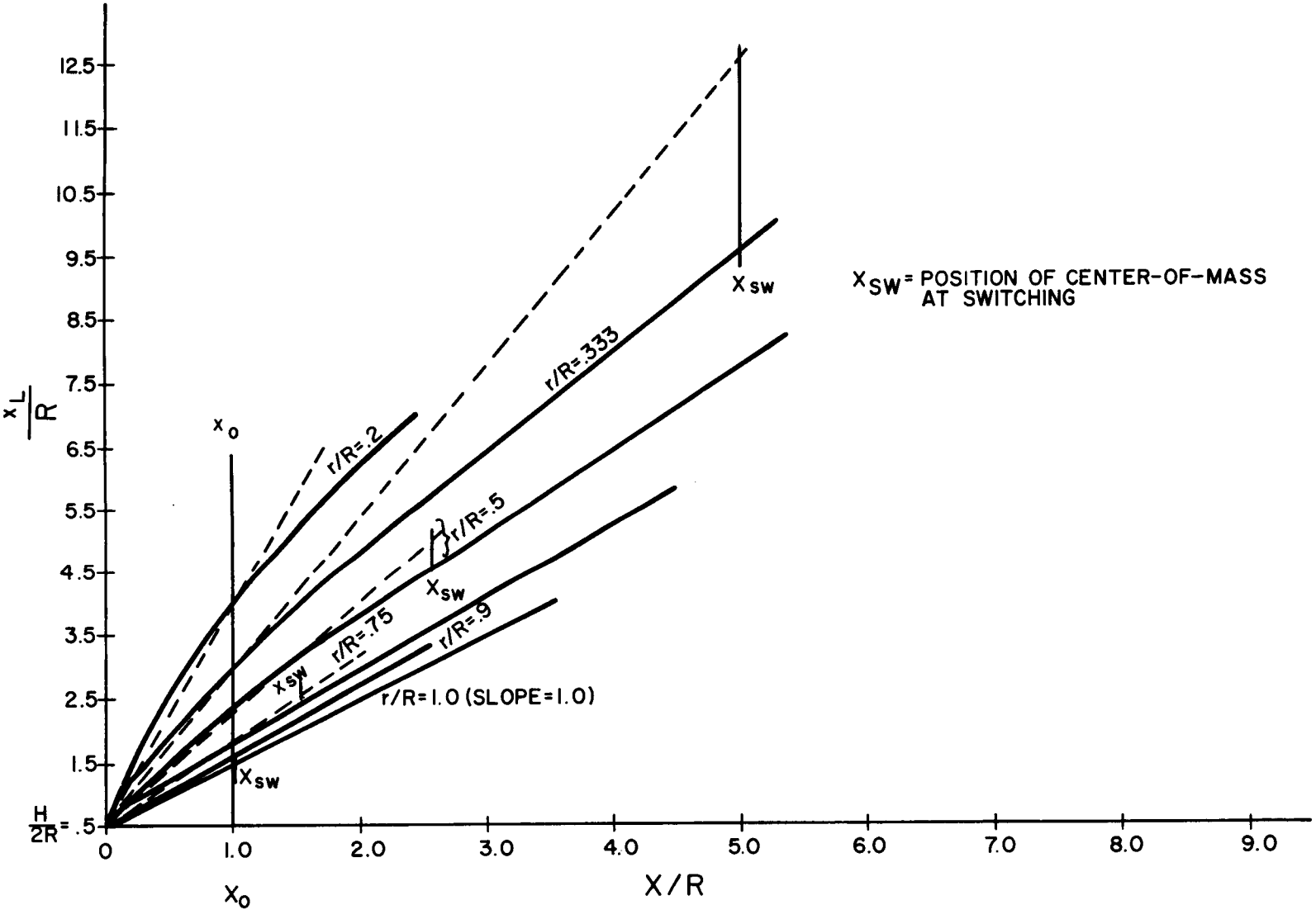

Figure A.7.-Leading surface position vs. center-of-mass position for several restriction sizes

The former assumes that the bead does not contract more than the restriction size while switching and the latter assumes incompressibility.

Accordingly, it can be deduced from Figure A.7 that:

(1) Equation (A.16) is a good, reasonable description of any switching process for large restriction sizes (i.e., $r/R > .75$).

(2) The dotted straight lines shown are good approximations to the solid lines for $x < x_0$ (geometric center).

Therefore, rather than involve the non-linearities of and undetermined deviations from the "squirt" switching model, the straight-line approximations are used in the text in analyzing the system characteristics.

These approximations should be extremely accurate for predicting the ambient acceleration field limit and the magnetomotive force required for switching, since only the initial x_L vs. x information is required. That is, these properties depend only on the largest rate of energy change and this occurs in the restriction.

The approximations are not so accurate for determining the switching time since significant variations occur before complete switching. Also, the approximations are not conservative (they tend to predict switching times less than the actual switching times), but still predict a reasonable estimate (i.e., within a factor of 2 for $r/R = .5$).

The straight-line approximation relating the bead's leading surface position to its center-of-mass position can be determined from Eq. (A.16) and is given by

$$x_L = \frac{H}{2} + \left\{\left[2\left(\frac{R}{r}-1\right)\left(\frac{H+L}{2}\right) - H\left(\frac{R}{r}+1\right) + \left[H^2\left(\frac{R}{r}+1\right)^2 + 4H\left[2\left(\frac{R}{r}\right)^3 - \left(\frac{R}{r}\right)^2 - 1\right]\left(\frac{H+L}{2}\right) + 4\left(\frac{R}{r}-1\right)^2\left(\frac{H+L}{2}\right)^2\right]^{\frac{1}{2}}\right] \Big/ 2\frac{R}{r}\left[1-\left(\frac{r}{R}\right)^3\right]\left[\frac{H+L}{2}\right]\right\} x \quad . \qquad (A.17)$$

Finally, the electromagnetic energy can be determined as a function of the bead's center-of-mass position by substituting Eq. (A.17) into Eq. (A.15):

$$U_B = U_{BO} + F_B x \tag{A.18}$$

where

$$U_{BO} = -\frac{1}{2}(NI)^2 \left\{ \left[\mu_o \left(1-\frac{r}{R}\right)(2R+L) \right] + \left[\mu_o \frac{r}{R}(2R+L) \right] \right.$$

$$\left. + \left[\frac{r^2}{R^2}(\mu_b-\mu_o) \Big/ \left\{ \frac{r}{R} + \frac{\mu_b}{\mu_o}\left(1-\frac{r}{R}\right) \right\} \right] \frac{H}{2} \right\} \tag{A.19}$$

and

$$F_B = \left[\frac{r^2}{R^2}(\mu_b-\mu_o) \Big/ \left\{ \frac{r}{R} + \frac{\mu_b}{\mu_o}\left(1-\frac{r}{R}\right) \right\} \right] \left\{ \left[2\left(\frac{R}{r}-1\right)\left(\frac{H+L}{2}\right) - H\left(\frac{R}{r}+1\right) \right. \right.$$

$$+ \left[H^2\left(\frac{R}{r}+1\right)^2 + 4H\left[2\left(\frac{R}{r}\right)^3 - \left(\frac{R}{r}\right)^2 - 1 \right]\left(\frac{H+L}{2}\right) \right.$$

$$\left. \left. \left. + 4\left(\frac{R}{r}-1\right)^2\left(\frac{H+L}{2}\right)^2 \right]^{\frac{1}{2}} \right] \Big/ \left\{ 2\frac{R}{r}\left[1-\left(\frac{r}{R}\right)^3 \right]\left[\frac{H+L}{2}\right] \right\} \right\} . \tag{A.20}$$

The electromagnetic energy is also affected by possible deviations in reluctance as the bead emerges from the restriction. But, this effect tends to offset the x_L vs. x deviations just mentioned. This can be shown by examining Eq. (A.15). Any deviation in reluctance would mean an effective increase in r and, hence, an increase in the stored electromagnetic energy, which, in turn, would reduce the switching time.

This effect can be examined quantitatively for the hypothetical switching process model shown in Figure A.8. This model reflects the minimum possible reluctance across the chamber as a function of the bead's leading surface.

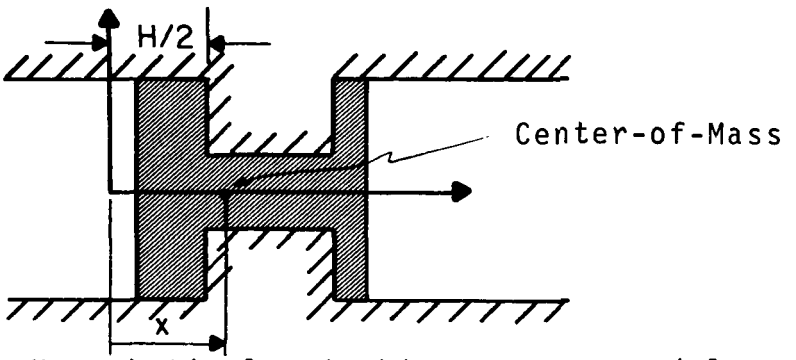

Figure A.8.-Hypothetical switching process model

After computing the effective reluctance in the restriction and right chamber as a function of the bead's leading surface, and placing into the energy Eq. (A.9), the electromagnetic energy becomes:

$$U_B = -\frac{1}{2}(NI)^2\left[\mu_o\left(1-\frac{r}{R}\right)L + \frac{\mu_o\mu_b rL}{\mu_o r + \mu_b(R-r)} - \mu_b L\right.$$

$$\left. + \mu_o(4R+L) + \left(\mu_b-\mu_o\right)x_L\right] \quad . \qquad (A.21)$$

In order to asses the effect of reluctance on switching time, the coefficients of x_L in Eqs. (A.21) and (A.15), which represent the energy rate of change, must be compared.

It is found that the coefficient of the hypothetical switching process is larger than that of the "squirt" switching process model by a factor of

$$\frac{R}{r} + \frac{\mu_b}{\mu_o}\left(\frac{R}{r}-1\right)\left(\frac{R}{r}\right) \quad .$$

According to the switching time equation in the text, this reduces the estimated switching time by a factor of approximately:

$$\sqrt{\frac{R}{r} + \frac{\mu_b}{\mu_o}\frac{R}{r}\left(\frac{R}{r}-1\right)} \quad .$$

This factor is shown in Table A.1 for different values of restriction sizes and permeability ratios.

This development was intended to show that the estimated switching time given by the "squirt" switching process model tends to be conservative and not intended to determine a minimum switching time. The switching time predicted by the "squirt" switching process model should provide a reasonable estimate for any practical switching system.

TABLE A.1

ELECTROMAGNETIC SWITCHING TIME FACTOR

r/R	μ_b/μ_o = 100	μ_b/μ_o = 200
1.0	1	1
.50	14	20
.33	25	35
.25	35	49

REFERENCES

A.1 Purcell, E. M.: Electricity and Magnetism. McGraw-Hill Book Co. (New York), 1962.

A.2 Seely, S.: Electromechanical Energy Conversion. McGraw-Hill Book Co. (New York), 1962.

A.3 Sommerfeld, A.: Electrodynamics. Vol. III, Academic Press (New York), 1964.

A.4 Harrington, R. F.: Introduction to Electromagnetic Engineering. McGraw-Hill Book Co. (New York), 1958.

A.5 Becker, R.: Electromagnetic Fields and Interactions. Vol. II, Blaisdell Publishing Company (New York), 1964.

APPENDIX B

DERIVATION OF SURFACE TENSION ENERGY MODEL AND APPROXIMATION

The energy expression for surface tension is given by

$$U_{ST} = \int \sigma dA_B + \text{constant} \qquad (B.1)$$

where U_{ST} is the potential surface energy, A_B is the surface area of the bead, and σ is the surface tension constant.

It may appear, at first, that the expression relating the surface area of the bead to its center-of-mass position is simply a geometric problem. A more thorough examination will reveal that the bead can exit the restriction with various profiles.

In this analysis, an energy model will be depicted for a certain type of switching process. It will then be shown that any practical switching process can be described reasonably well by this model. Finally, a linear approximation will be fitted to the model to allow simple yet credulous analysis of the system characteristics.

Consider the bead shown in Figure B.1. The menisci of the bead are assumed flat to permit an uncomplicated description of the bead's surface area. Furthermore, the thermodynamic criterion of marginal stability states that variations in the meniscus shape produce no variations in the total potential energy (ref. B.3).

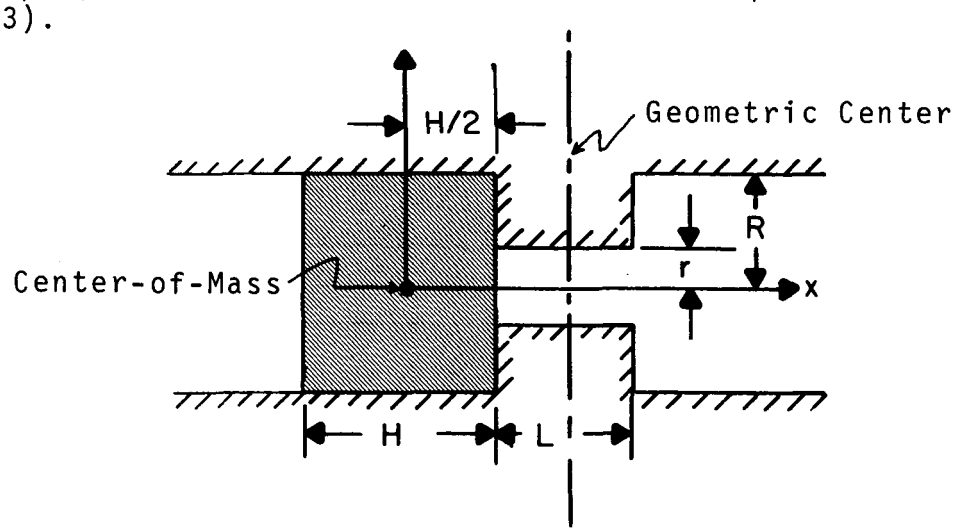

Figure B.1.-Bead configuration

The origin of the coordinate system is established at the bead's initial center-of-mass position when the bead is just about to enter the restriction.

The relationship between the surface area and the center-of-mass position of the bead as it proceeds through the restriction, as shown in Figure B.2, is given by:

$$A_B = 2\pi R(R+H) + \frac{\pi R\left(\frac{R}{r}-1\right)}{\left(\frac{R}{r}\right)^3 - 1}\left\{2\left(\frac{R}{r}-1\right)x - H\left(\frac{R}{r}+1\right)\right.$$

$$+ \left[H^2\left(\frac{R}{r}+1\right)^2 + 4H\left[2\left(\frac{R}{r}\right)^3 - \left(\frac{R}{r}\right)^2 - 1\right]x\right.$$

$$\left.\left. + 4\left(\frac{R}{r}-1\right)^2 x^2\right]^{\frac{1}{2}}\right\} \quad . \qquad (B.2)$$

This relationship is derived by first relating the surface area to the leading and trailing surfaces of the bead; relating the center-of-mass position to the leading and trailing surfaces; imposing the constant volume constraint; and finally, combining these expressions.

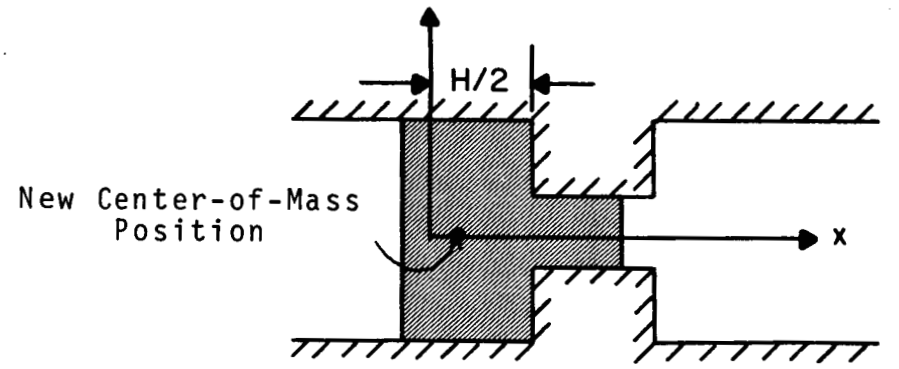

Figure B.2.-Bead proceeding through restriction

Now consider the bead as it exits the restriction. If the bead were forced strongly to switch, the switching process would resemble the "squirt" model shown in Figure B.3. Only during this type of switching process could the bead attain its maximum energy (area) state. Obviously the area relationship of Eq. (B.2) still applies here.

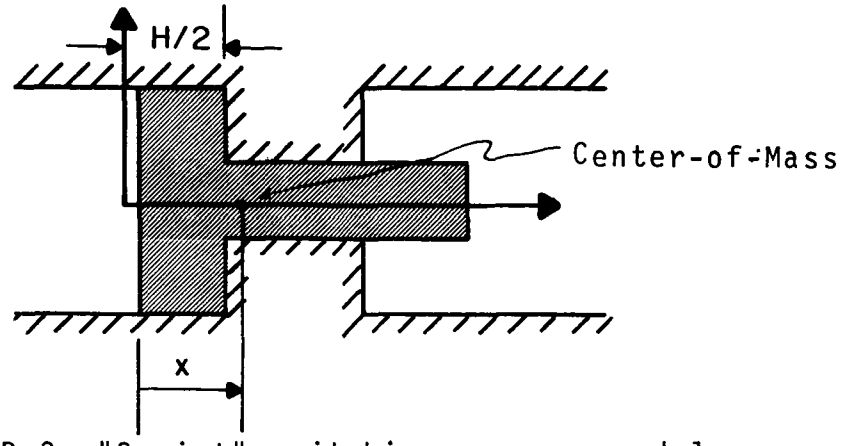

Figure B.3.-"Squirt" switching process model

Now, rather than trying to depict deviations from the "squirt" switching process physically, it is more convenient and apropos to examine deviations from a plot of the "squirt" switching process [Eq. (B.2)], which is shown as the solid line in Figure B.4. The surface area of the bead, A_B, normalized with respect to its initial area, A_O, is the ordinate, and the center-of-mass position, normalized with respect to R, is the abscissa.

Because of the symmetry of the system, the complete single switching process is shown symmetrical about the geometric center.

The solid line describes any switching process as the leading surface of the bead proceeds through the restriction. Only when the bead begins to emerge from the restriction can deviations occur. The shaded portion for each respective restriction represents the possible deviations from Eq. (B.1) for that restriction, as the bead emerges from the restriction.

In effect, the minimum value of each shaded portion represents the minimum possible surface area (energy) of the bead at switching for the particular restriction. It is the area of the bead when the leading surface just begins to emerge from the restriction, as shown in Figure B.5.

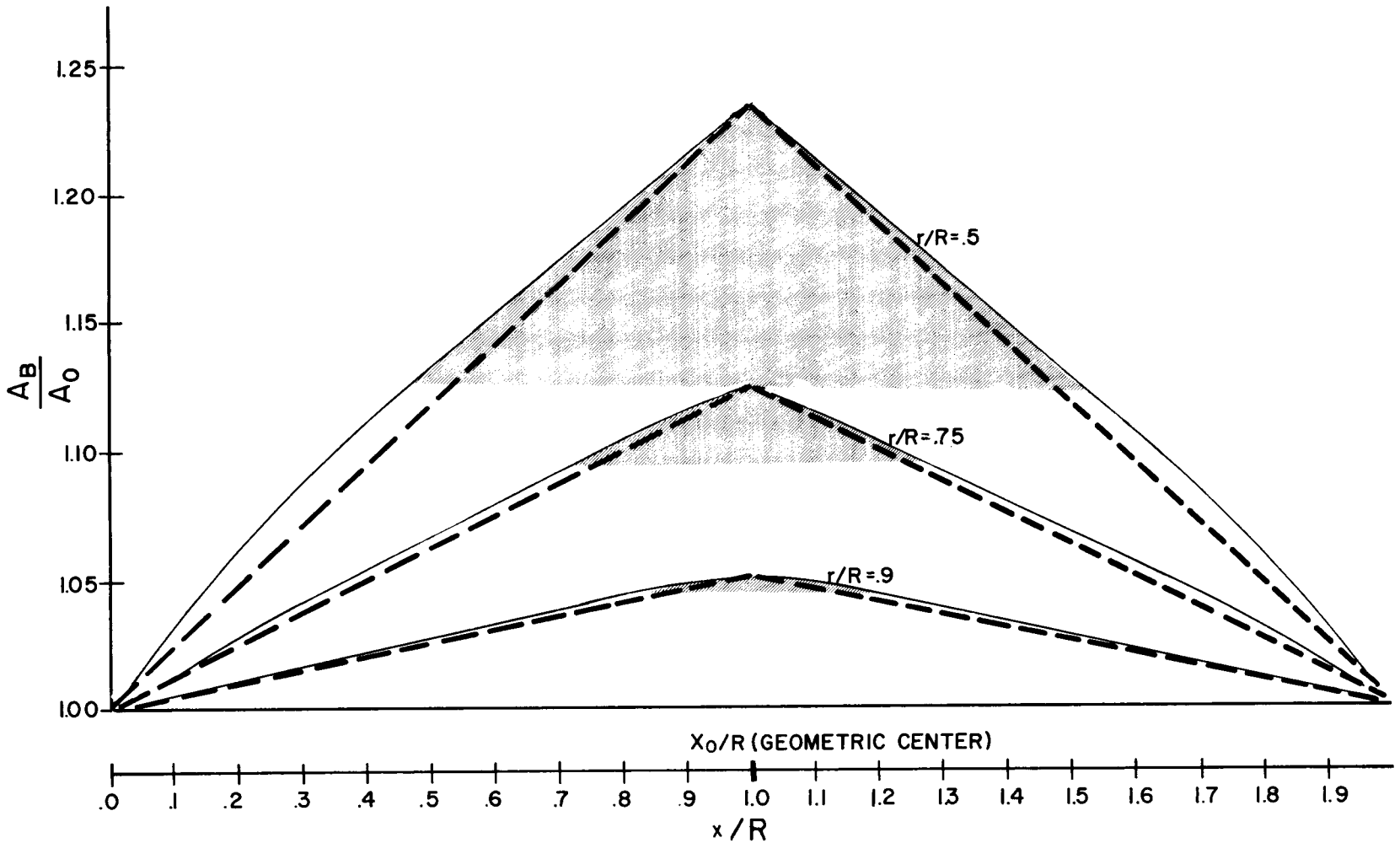

Figure B.4.-Surface area vs. center-of-mass position for different restriction sizes

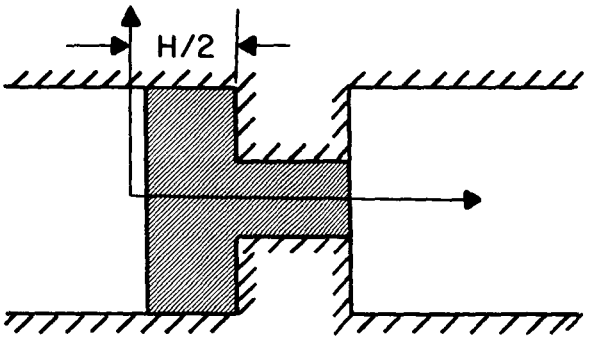

Figure B.5.-Representation of the minimum possible area that the bead can have at switching

It is apparent from Figure B.4 that:

(1) Equation B.2 is a good reasonable description of any switching process for large restrictions (i.e., $r/R > .75$).

(2) The dotted straight lines shown are good approximations to the solid lines.

Hence, rather than involve the non-linearities of and undetermined deviations from Eq. (B.2), the straight-line approximations are used in the text to analyze the system characteristics. These approximations are especially warranted in determining the ambient acceleration field limit, and magnetomotive force required for switching, since these properties depend only on the largest rate of energy change and this occurs in the restriction.

While not entirely as accurate for determining the switching time, the straight-line approximation does tend to give a reasonable, conservative estimate.

Using Eqs. (B.2) and (B.1), the straight-line approximation relating the surface energy of the bead to its center-of-mass position becomes:

$$U_{ST} = U_{STO} + F_{ST}x \qquad x \leq x_o \qquad (B.3)$$

$$= \bar{U}_{STO} - F_{ST}x \qquad x \geq x_o$$

where

$$U_{STO} = 2\pi R\sigma(R+H) \qquad (B.4)$$

$\bar{U}_{STO}$ = energy constant determinable from Figure B.4

$$F_{ST} = \frac{2\pi R\sigma\left(\frac{R}{r}-1\right)}{\left(\frac{R}{r}\right)^3 - 1}\left\{\left(\frac{R}{r}-1\right) - \frac{H\left(\frac{R}{r}+1\right)}{H+L} + \left[H^2\left(\frac{\frac{R}{r}+1}{H+L}\right)^2\right.\right.$$

$$\left.\left. + \frac{2H}{H+L}\left[2\left(\frac{R}{r}\right)^3 - \left(\frac{R}{r}\right)^2 - 1\right] + \left(\frac{R}{r}-1\right)^2\right]^{\frac{1}{2}}\right\} \qquad (B.5)$$

and

$$x_o = \frac{H+L}{2} = \text{geometric center.} \qquad (B.6)$$

It is interesting to note that the "squirt" switching model curves begin to decrease for large x/R, as r/R becomes less than .25. This effect is shown in Figure B.6. What this means is that the center-of-mass of the bead is now more affected by the large moment arm of the mass past the restriction than by the mass remaining behind in the chamber.

Also, note that the initial slopes of all the switching model curves continue to increase for decreasing values of r/R. These slopes determine the magnetomotive force required for switching and the ambient acceleration field limit and, to a great extent, the switching time. The monatonic nature of these slopes suggests that the "squirt" model is valid for all restrictions. However, since the initial slope information is lost completely in the approximation, it must be concluded that the properties of the switching system determined in the text are not valid for $r/R < .25$.

It remains, though, that the switching model curves are theoretically correct for all restrictions under the assumptions stated (i.e., no friction, hysteresis, etc.).

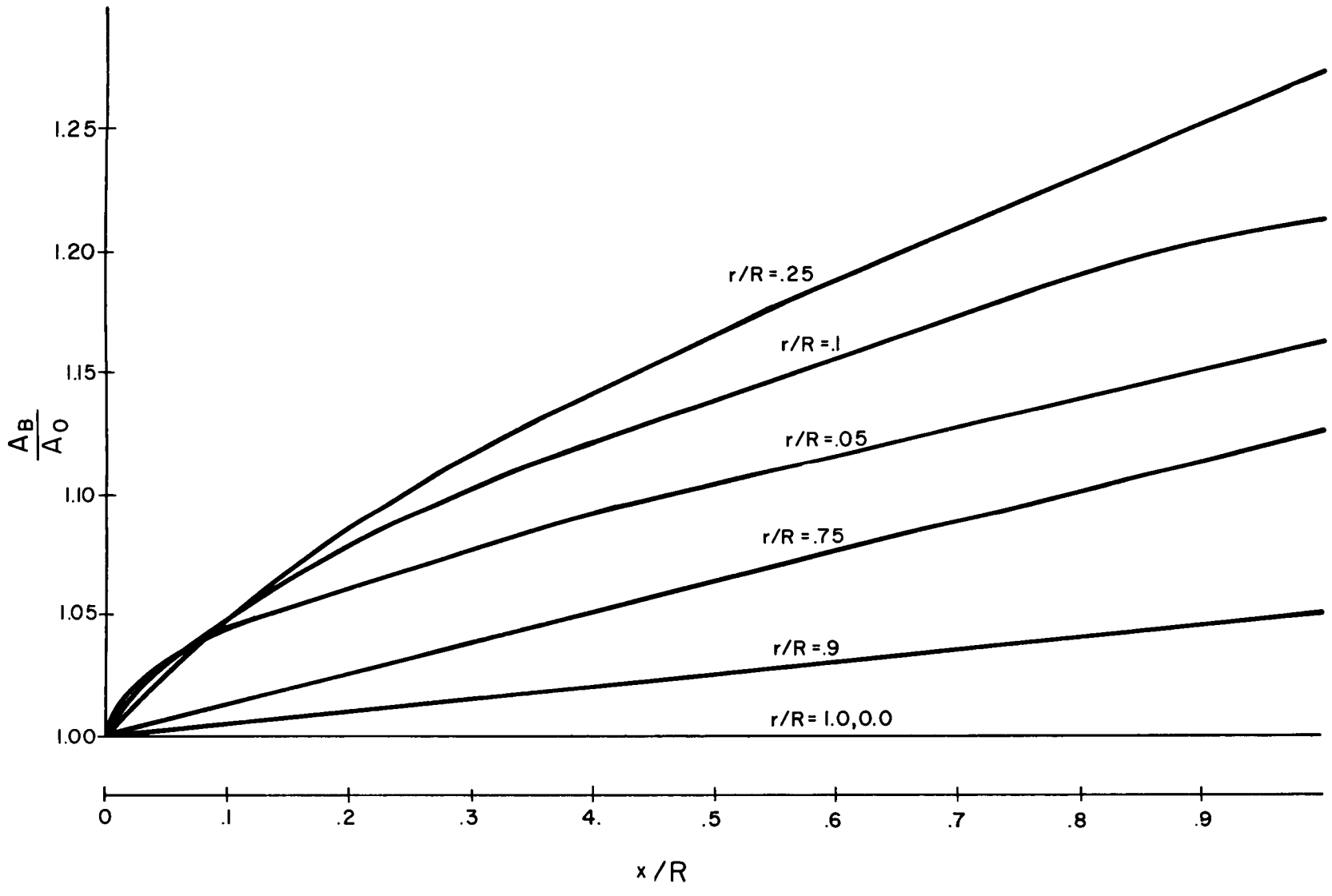

Figure B.6.-Surface area vs. center-of-mass position showing effect of small restriction sizes

REFERENCES

B.1 Zisman, W. A.: Relation of Equilibrium Contact Angle to Liquid and Solid Constitution. Advances in Chemistry, Series 43, pp. 1-52, 1964.

B.2 Sharpe, L. H.; and Schonhorn, H.: Surface Energetics, Adhesion, and Adhesive Joints. Advances in Chemistry, Series 43, pp. 189-200, 1964.

B.3 Reynolds, W. C.; Satterlee, H. M.: Liquid Propellant Behavior at Low and Zero G. The Dynamic Behavior of Liquids in Moving Containers, NASA SP-106, Chapter 11, 1966.

B.4 Rose, R.; Shepard, L. A.; and Wulff, J.: The Structure and Properties of Materials. Vol. IV, John Wiley & Sons, Inc. (New York), 1966.

National Aeronautics and Space Administration

Electronics Research Center

Cambridge, Massachusetts, April 1968

125-19-05-02